Materials Science Forum Vols. 111 - 112 (1992) pp. 53-62

MODELLING LOCAL MASS-TRANSFER CONTROLLED CORROSION AT GEOMETRICAL IRREGULARITIES

J. Postlethwaite, S. Nesic and G. Adamopoulos
Department of Chemical Engineering, University of Saskatchewan, Saskatoon, Saskatchewan, S7N 0WO, Canada

ABSTRACT

A low Reynolds number (LRN), k-ϵ, turbulence model has been used to extend the validity of a standard k-ϵ turbulence model deep into the viscous sublayer which is important for modelling mass transfer controlled corrosion in aqueous flow systems at high Schmidt numbers where the bulk of the resistance to mass transfer is embedded deep within the viscous sublayer.

The model has been applied to a study of the local mass transfer and corrosion rates at a sudden pipe expansion, a sudden pipe constriction and a groove in a pipe.

INTRODUCTION

The corrosion of metals in aqueous solutions is often mass-transfer controlled (1,2). Many of the most severe flow system corrosion problems occur at geometrical irregularities (3,4) under conditions of complex flow including secondary flow at bends and flow separation with recirculation and reattachment at sudden expansions and contractions. The wall mass transfer rates under complex flow conditions may be determined by experiment (5) or determined from a simultaneous solution of the time averaged continuity, momentum and species mass transport equations.

In a recent erosion-corrosion study (6) the rate of mass transfer of oxygen was determined on the basis of a correlation based on the results of Sydberger and Lotz (5). It was found that the electrochemical mass transfer results of Sydberger and Lotz for a sudden expansion could be correlated with the local near wall turbulence levels predicted with a k-ϵ eddy viscosity model (EVM). There was however concern regarding the generality of the model. Further, the implementation of the k-ϵ turbulence model at the wall used the wall function (WF) approach which is strictly incorrect for separated and recirculating flows.

This paper presents a more general model for the prediction of wall mass transfer rates under disturbed flow conditions. The hydrodynamic code was revised to include a low Reynolds number (LRN) k-ϵ model. Unlike the WF approach a LRN closure attempts to model the turbulent transport across the entire near-wall region. This is especially important for predicting mass transfer at the wall, since the mass transfer boundary lager, for aqueous flows with high Schmidt numbers, is embedded within the hydrodynamic viscous sublayer. The small amount of turbulence in the viscous sublayer whilst unimportant from a hydrodynamic standpoint is very important for mass transport under conditions where the kinematic viscosity is very much larger than the molecular diffusivity (7).

THE MODEL

The turbulence model is based on the standard, k-ϵ, EVM model of Launder and Spalding (TEACH) (8). In the present study the mass transfer is modelled by assuming an analogy in the mechanisms of turbulent momentum and mass transport, via the turbulent Schmidt number concept (9).

A solution is sought for a set of elliptical partial differential conservation equations that all have the same form. In cylindrical co-ordinates:

$$\frac{\partial}{\partial x}(\rho U\Phi) + \frac{1}{r}\frac{\partial}{\partial r}(r\rho V\Phi) = \frac{\partial}{\partial x}\left(\Gamma_\Phi \frac{\partial \Phi}{\partial x}\right) + \frac{1}{r}\frac{\partial}{\partial r}\left(r\Gamma_\Phi \frac{\partial \Phi}{\partial r}\right) + S_\Phi \qquad (1)$$

where $\Phi = U, V, k, \epsilon, m, \ldots$

The governing equations for flow and mass transfer are represented in Table 1.

Table 1: Conservation equations

Conservation of	Φ	Γ_Φ	S_Φ
Mass	1	0	0
Axial momentum	U	μ_{eff}	$\frac{\partial}{\partial x}(\mu_{eff}\frac{\partial U}{\partial x}) + \frac{1}{r}\frac{\partial}{\partial r}(r\mu_{eff}\frac{\partial V}{\partial x}) - \frac{\partial p}{\partial x}$
Radial momentum	V	μ_{eff}	$\frac{\partial}{\partial x}(\mu_{eff}\frac{\partial U}{\partial r}) + \frac{1}{r}\frac{\partial}{\partial r}(r\mu_{eff}\frac{\partial V}{\partial r}) - 2\mu_{eff}\frac{V}{r^2} - \frac{\partial p}{\partial r}$
Turbulent kinetic energy	k	$\frac{\mu_{eff}}{\sigma_k}$	$P_k - \rho\epsilon$
Turbulent dissipation rate	ϵ	$\frac{\mu_{eff}}{\sigma_\epsilon}$	$\frac{\epsilon}{k}(C_{\epsilon 1}f_1 P_k - C_{\epsilon 2}f_2\rho\epsilon)$
Species	m	ρD_{eff}	0

$$P_k = \mu_{eff}\{2[(\tfrac{\partial U}{\partial x})^2 + (\tfrac{\partial V}{\partial r})^2 + (\tfrac{V}{r})^2] + (\tfrac{\partial U}{\partial r} + \tfrac{\partial V}{\partial x})^2\}$$

The effective viscosity μ_{eff} and diffusivity D_{eff} are the sum of the molecular an turbulent contributions;

$$\mu_{eff} = \mu + \mu_t \qquad (

$$D_{eff} = \frac{\mu}{\rho Sc} + \frac{\mu_t}{\rho \sigma_t} \qquad (3)$$

effective molecular turbulent

Following Milojevic, Borner and Durst (10) a set of well established constants were used.

$$C_\mu = 0.09, \quad C_{\epsilon 1} = 1.44, \quad C_{\epsilon 2} = 1.92$$

$$\sigma_k = 1.0, \quad \sigma_\epsilon = 1.3, \quad \sigma_t = 0.9$$

The value of the turbulent Schmidt number $\sigma_t = 0.9$, which is of special importance in mass transfer studies, is according to Kays and Crawford (9), constant throughout the bulk of the fluid, especially for fluids with high molecular Schmidt numbers. Measurements have indicated that very close to the wall within the viscous sublayer, the value of σ_t approximately doubles. A value of 1.7 was used in the present study in this region (9).

For the boundary conditions, the previously used WF approach (6) was substituted with a LRN model (11,12). Turbulence damping functions used in the near wall regions are those of Lam and Bremhorst (12).

$$f_\mu = [1 - \exp(-0.0165\, Re_y)]^2 \left(1 + \frac{20.5}{Re_T}\right) \qquad (4)$$

$$f_1 = 1 + \left(\frac{0.05}{f_\mu}\right)^3 \qquad (5)$$

$$f_2 = 1 - \exp(-Re_T^2) \qquad (6)$$

$$\text{where } Re_y = \frac{\rho y \sqrt{k}}{\mu} \qquad Re_T = \frac{\rho k^2}{\mu \epsilon}$$

The WF approach which bridges over the viscous sublayer with a universal velocity profile misses important features of the mass transfer boundary layer deeply embedded within it. Instead, a turbulence model is required which can penetrate deep into the hydrodynamic boundary layer, at the same time accounting for the changes in the turbulence structure due to the wall. This suggests that a LRN approach, which enables the extension of the k - ϵ turbulence model all the way to the wall, should be used in the case of modelling mass transfer in aqueous flow.

For purely hydrodynamic LRN models it is usually adequate to place the first node adjacent to the wall somewhere in the viscous sublayer ($y^+ < 5$), typically $y^+ \approx 1$. However, in the case of mass transfer at high Schmidt numbers (Sc $\approx$ 1000), the thickness of the diffusion mass transfer boundary layer is approximately one tenth

the viscous sublayer. Therefore, the first node was placed at $y^+ \approx 0.1$. The final solution fields have shown that only at these distances from the wall does the level of turbulent transport of mass become negligible compared to the molecular diffusional component.

The solution of the species mass transport equations gives the concentration field of the species under consideration; ferricyanide or dissolved oxygen for example. The local transport flow of the species is determined from a knowledge of the diffusion coefficient and the species concentration at the node closest to the wall. Limiting conditions, are assumed, i.e. the wall concentration is set at zero, and the sole mode of transport is assumed to be molecular diffusion. The mass transfer coefficient, k', is then calculated using the local transport flow and the overall concentration difference between the bulk solution and the wall.

SIMULATION RESULTS

Mass Transfer

The predictions of the present model and the experimental mass transfer results of Sydberger and Lotz (5) for a sudden pipe expansion and a sudden pipe constriction are presented below. The electrochemical mass transfer measurements of Sydberger and Lotz involved a solution of the reduction of ferricyanide with a Schmidt number of 1460.

The predictions and the measured values of the wall mass-transfer coefficients for the sudden pipe expansion, Figure 1, have a similar profile and both approach the values given by the Berger-Hau (13) straight pipe correlation downstream of the flow reattachment point.

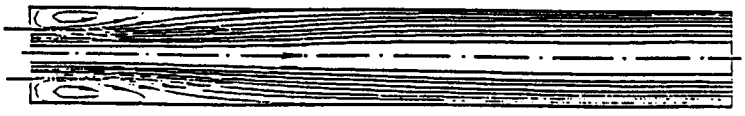

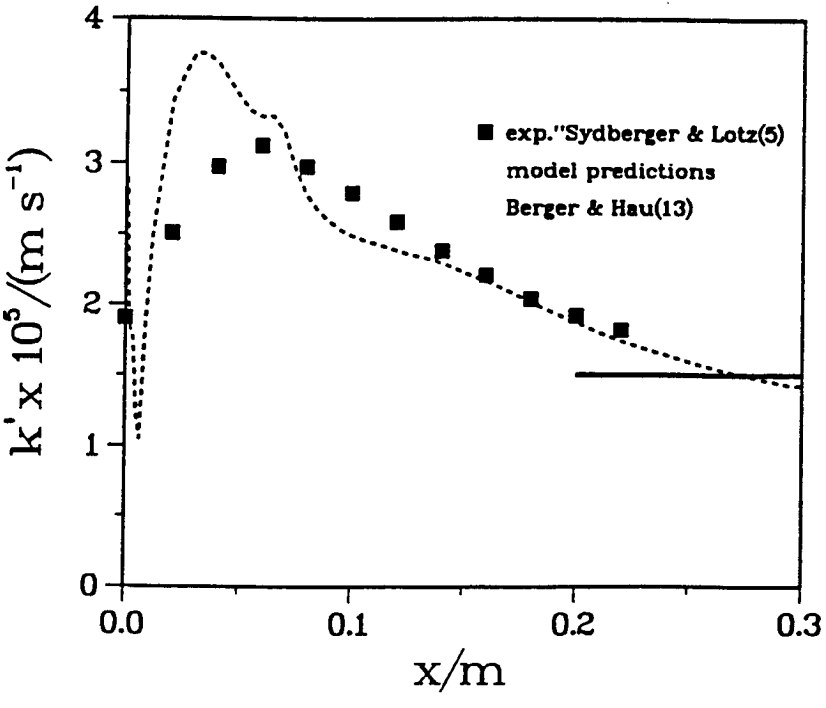

Figure 1 Model predictions and experimental mass transfer coefficients at the walls of a sudden pipe expansion, 20 mm diamter inlet, 40 mm diamter outlet. Re, in 40 mm tube, = 21,000.

The predictions for the streamlines and kinetic energy of turbulence field for the sudden expansion are given in Figure 2. From the kinetic energy of turbulence field it is clear that the turbulence created by the sudden expansion is carried downstream resulting in maximum near-wall turbulence and mass transfer in the region near the flow reattachment point.

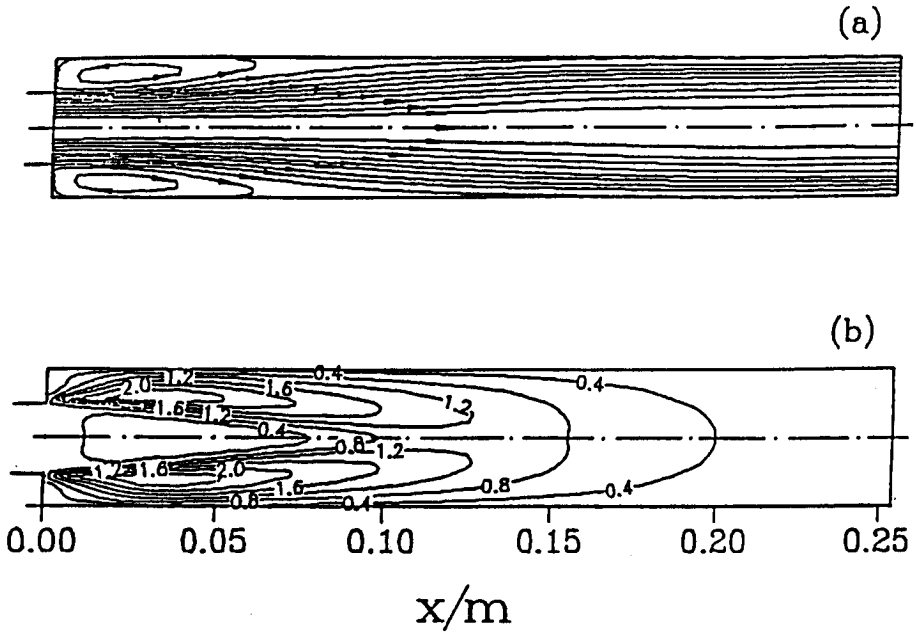

Figure 2 Flow steamlines and kinetic energy of turbulence field at a sudden pipe expansion, 20 mm diameter inlet, 40 mm diameter outlet. Re, in 40 mm tube, = 21,000

An example of the change in the effective viscosity and the effective diffusivity with the distance from the wall are shown in Figure 3.

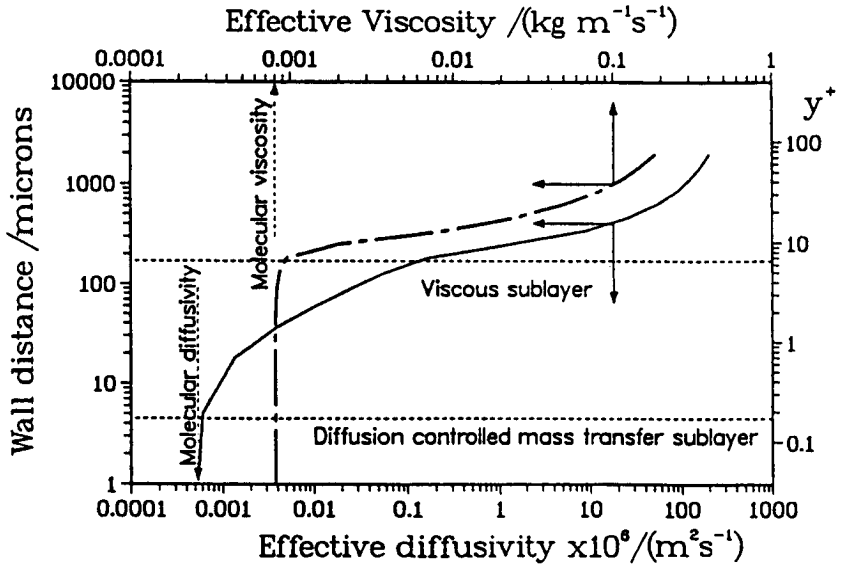

Figure 3 Momentum and mass transport coefficients, μ_{eff} and D_{eff} at a point downstream of the flow reattachment point at a sudden expansion. Flow conditions as in Figure 2.

The corresponding velocity and concentration profiles are shown in Figure 4.

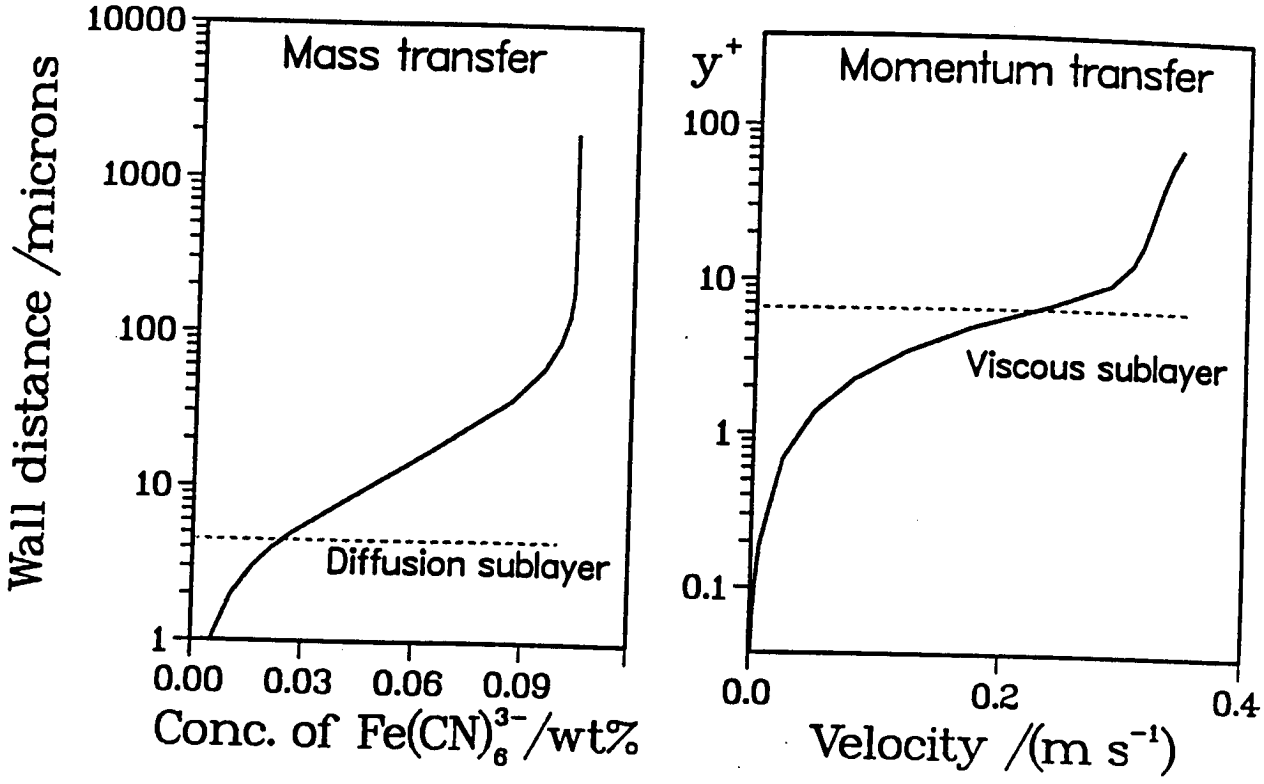

Figure 4 Velocity and concentration profiles at a sudden pipe expansion, under conditions of Figure 3.

The results in Figure 3, illustrate why for purely hydrodynamic LRN models it is usually adequate to place the first node adjacent to the wall somewhere in the viscous sublayer ($y^+<5$), typically $y^+\approx1$. For mass transfer simulations with high Schmidt numbers (≈1000) the thickness of the molecular diffusion controlled portion of the mass transfer boundary layer is much less and a value of $y^+ = 0.1$-0.2 was used for the placement of the first node.

The predictions for the sudden pipe contraction, Figure 5, are in substantial agreement with the measurements of Sydberger and Lotz; with the maximum mass transfer rates corresponding to the "leading edge" of the constriction as might be expected.

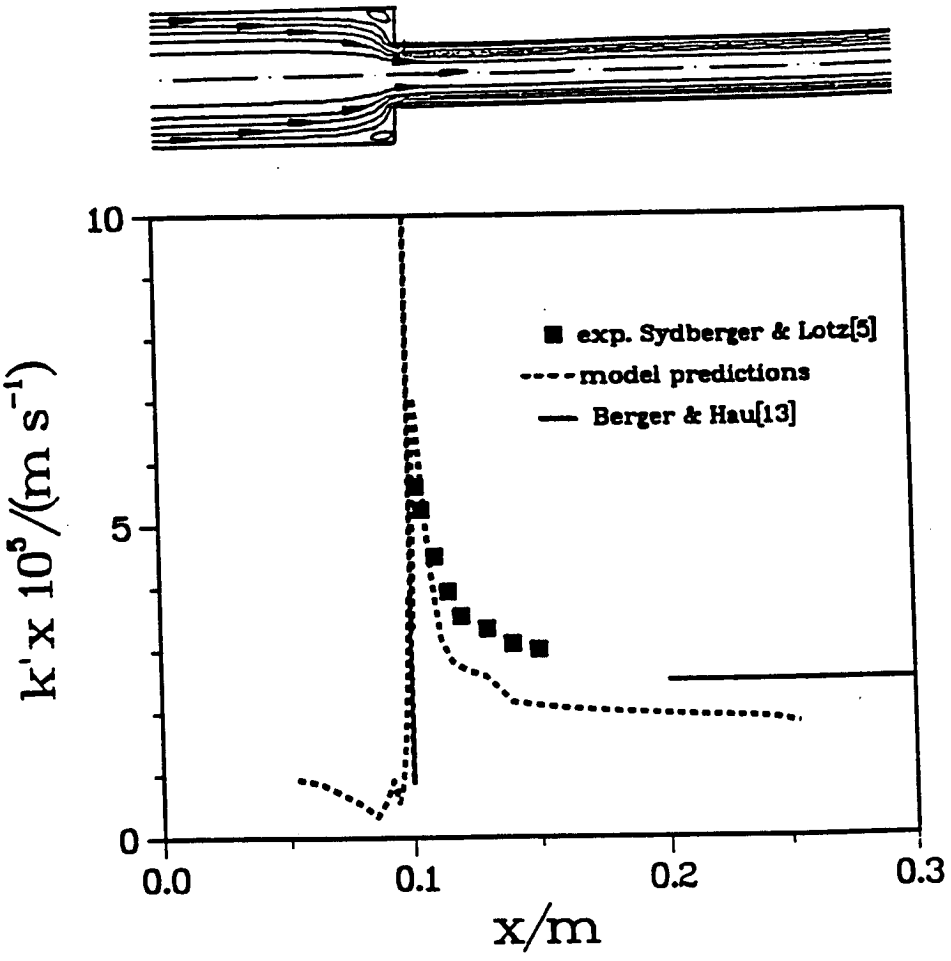

Figure 5 Model predictions and experimental mass transfer coefficients for a sudden pipe constriction, from 40 mm to 20 mm. Re, in 20 mm section, = 21,000

Corrosion

Simulations of oxygen mass-transfer controlled corrosion in the absence of surface films and with partial coverage are presented below. In these simulations the rate of corrosion was determined only at the film free surfaces. It would be relatively simple to add the corrosion rate in the "filmed" areas providing some estimate of the film thickness and the resistance to diffusion of oxygen through the film in question were available.

The corrosion rate profile for a groove in a film free carbon steel pipe is shown in Figure 6. The very high corrosion rates relate to the high velocity of 15 m/s used in this simulation.

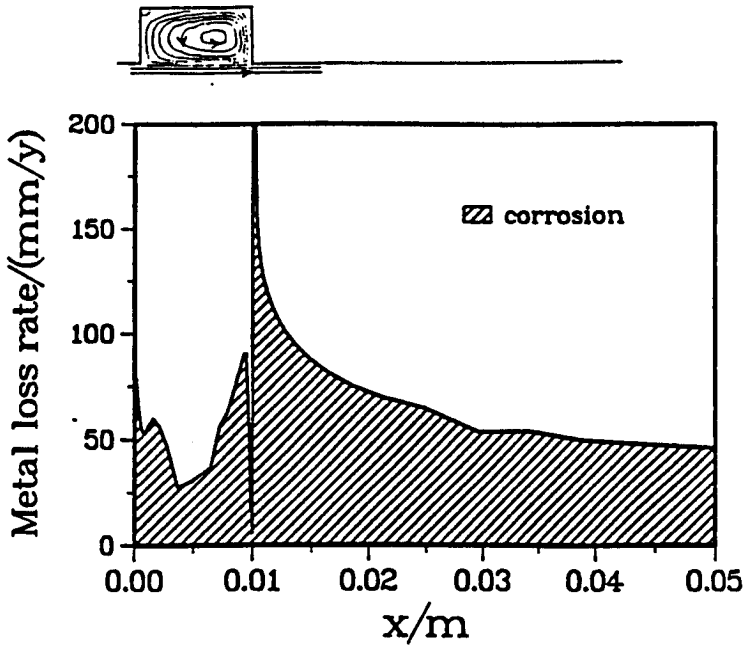

Figure 6 Model predictions for the corrosion rate profile at a 10 x 10 mm groove in a 100 mm diameter pipe, velocity = 15 m/s. Oxygen mass-transfer controlled corrosion of carbon steel pipe.

The corrosion predictions for a sudden pipe (carbon steel) expansion are compared with the experimental results of Lotz and Postlethwaite (14) in Figure 7. These results which have been discussed were fully contained in a small erosion component, which is not shown in Figure 7, relating to the fact that a dilute sand slurry was the medium under study.

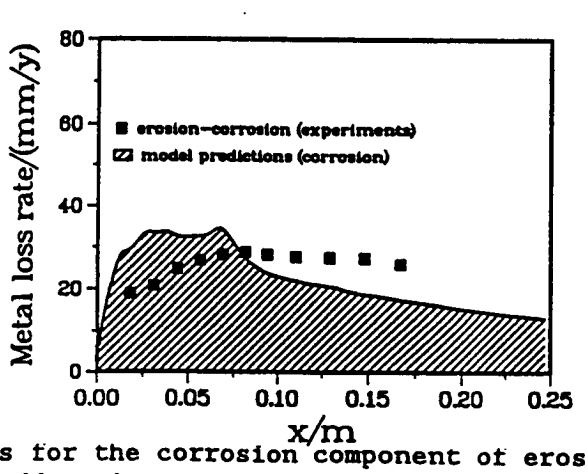

Figure 7 Model predictions for the corrosion component of erosion-corrosion at a sudden pipe expansion from 21.1 mm to 42.5 mm carrying a dilute sand slurry at a velocity of 13.2 m/s in the 21.1 mm section, and experimental erosion-corrosion results of Lotz and Postlethwaite (14).

The effect of partial film removal which is found in many instances of flow induced corrosion is illustrated in Figure 8. The simulation is for a sudden pipe expansion with small areas of film removed, one in the recirculation zone and the other downstream of the flow reattachment point.

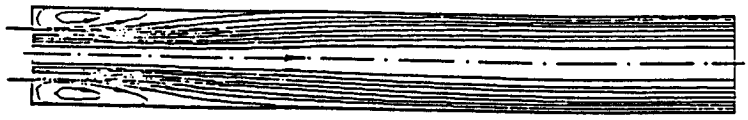

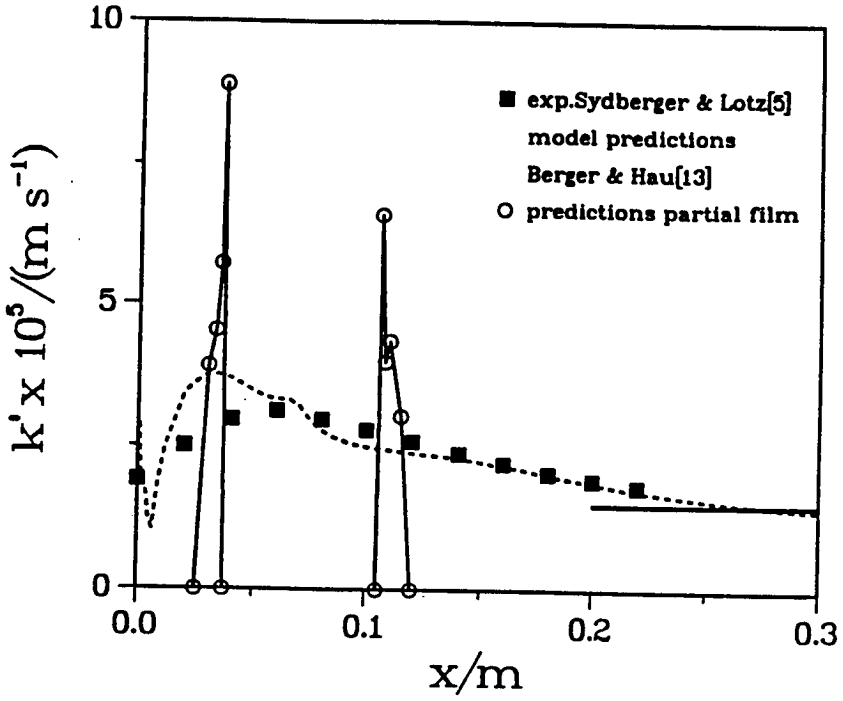

Figure 8 Model predictions for mass transfer coefficients under conditions given in Figure 1, but with surface film over all but two bare patches, one upstream of the flow reattachment point and one downstream.

CONCLUSIONS

1. The rate of local mass transfer controlled corrosion under disturbed flow condition at geometrical irregularities, in axisymetric systems, can be readily modelled by the application of a 2-D, low Reynolds number, k-ϵ, turbulent flow and mass transfer model.

2. The method can be adapted to account for the situation where only small portions of a protective film have been removed by the effect of flow.

REFERENCES

1. J. Postlethwaite, M.H. Dobbin and K. Bergevin, Corrosion 42, 514-421 (1986)
2. B.K. Mahato, S.K. Voota and L.W. Shemilt, Corrosion Science, 8, 173-193 (1968)
3. E. Heitz, Corrosion/90, Paper No 1, (Houston, TX: NACE, 1990)
4. E.D.D. During (compiler), Corrosion Atlas, Vol 1 and 2. Elsevier (1988)
5. T. Sydberger and U. Lotz, J. Electrochem. Soc., 129, 276-283 (1982)

6. S. Nesic and J. Postlethwaite, Can. J. Chem. Eng., 69, June (1991)
7. C.S. Lin, E.B. Denton, H.S. Gaskill and G.L. Putman, Ind. Eng. Chem., 43, 2136-2143 (1951)
8. B.E. Launder and D.B. Spalding, Comp. Methods Appl. Mech. and Engng., 3, 269-289 (1974)
9. W.M. Kays and M.E. Crawford, Convective Heat and Mass Transfer, McGraw Hill, (1980), p. 225-229
10. D. Milojevic, T. Borner and F. Durst, Prediction of turbulent gas-particle flow measurements in a plain confined jet, World Congress Particle Technology, Part IV, Partikel Technologie Nurnberg, W. Germany (1986)
11. W.P. Jones and B.E. Launder, Int. J. Heat Mass Transfer 16, 1119-1130 (1973)
12. C.K.G. Lam and K. Bremhorst, ASME J. Fluids Eng, 103, 456-460 (1981)
13. F.P. Berger and K.-F.F.-L. Hau, Int. J. Heat Mass Transfer 20, 1185-1194 (1977)
14. U. Lotz and J. Postlethwaite, Corrosion Science, 30, 95-106 (1990)

NOTATION

C_μ, C_1, C_2 - constants in the k - ϵ model of turbulence
f_μ, f_1, f_2 - constants in the LRN turbulence model

$k = \frac{1}{2}\overline{u_i u_i}$ - kinetic energy of turbulence
k - mass transfer coefficient
m - species mass concentration
P_k - production of k
p - pressure
r - radial coordinate
Re - Reynolds number
$Re_y = \frac{\rho y\sqrt{k}}{\mu}$ - turbulence Reynolds number
$Re_T = \frac{\rho k^2}{\mu\epsilon}$ - turbulence Reynolds number
u,v - components of the fluctuation velocity vector
U,V - components of mean velocity vector
U^+ - nondimensional velocity
S - source term
Sc - Schmidt number
x - axial coordinate
y - distance from the wall
y^+ - nondimensional distance from the wall

Greek Letters

Γ - diffusion coefficient

$\epsilon = \frac{2\mu}{\rho}\overline{s_{ij}s_{ij}}$ - dissipation of kinetic energy of turbulence
Φ - general variable
μ - dynamic viscosity
$\mu_t = C_\mu f_\mu \frac{\rho k^2}{\epsilon}$ - turbulent viscosity
ρ - fluid, density
$\sigma_k, \sigma_\epsilon, \sigma_t$ - turbulent Schmidt numbers

Subscripts

eff - refers to effective value (molecular + turbulent)
k - refers to kinetic energy of turbulence
t - refers to turbulent value
ϵ - refers to dissipation of kinetic energy of turbulence
Φ - refers to general variable